

# Internal heat transfer in Czochralski grown silicon crystals

John P. Wallace

Castling Analysis Corp., Weyers Cave, Virginia 24486

John K. Tien and Jerry A. Stefani

Center for Strategic Materials, Henry Krumb School of Mines, Columbia University New York, New York 10027

Kwang Su Choe

IBM Corporation, East Fishkill Facility, Hopewell Junction, New York 12533

(Received 2 October 1989; accepted for publication 17 September 1990)

Silicon crystals grown by the CZ process have recently been studied with eddy current techniques to determine thermal profiles within the growing crystal. A key question concerning heat transfer in this semiconductor system during CZ growth is whether optical semitransparency in the infrared is important in affecting the high-temperature thermal distribution within the crystal. From normal Fourier's law calculations, well behaved profiles with rather flat radial isotherms are predicted in CZ growth. Eddy current data, though, show abrupt temperature changes near the crystal outer surface, indicating sharp radial thermal gradients. It is proposed that these sharp gradients are due in part to the onset of optical semitransparency in the crystal in the infrared. It is expected that such a transparency phenomenon will occur below a transition temperature. Any sharp gradients can be responsible for creep damage during growth.

Recently a multifrequency eddy current probe has been incorporated into a Czochralski crystal grower in order to monitor thermal profiles within a growing crystal.<sup>1-4</sup> Silicon was chosen because it is one of the best understood and characterized materials. Eddy currents were chosen to monitor temperature because thermocouples are not easily introduced into a crystal. When silicon is semitransparent, an opaque thermocouple would not be a reliable measure of temperature because it can preferentially absorb radiation. The data that were collected suggests that conductive heat transfer within the crystal is not sufficient to explain the history of thermal profiles during growth. With the peak of the black-body spectrum well below the band gap energy of silicon, the number of thermally activated free carriers determines the optical depth and efficiency of the infrared radiative heat transfer within the crystal. The question we are asking is whether silicon upon cooling and becoming semitransparent will show any significant changes in internal heat transfer due to radiative heat transfer. Silicon, because of its high refractive index, will make the free surface of the crystal play a role in any internal radiant heat transfer. If the near surface region has cooled so that the material is nearly transparent the surface becomes an excellent internal reflector for radiant energy coming from within the material. With a refractive index of 3.4 which produces a Brewsters angle of 17.4 deg of arc, that results in a minimum of 96% internal reflection from an isotropic internal radiant source. There are secondary effects determined by the gradient of the refractive index on radiation moving parallel to the surface, but they are minor compared to the efficiency of a cool surface as a reflector.

An eddy current technique has been used to determine temperature profiles in growing silicon crystals by means of monitoring a weak induced electromagnetic field interacting with the semiconductor, an interaction which alters the in-

duced field measurably so that electrical conductivity values can be determined.<sup>1-4</sup> Employing the known intrinsic electrical behavior of silicon, conductivity values can then be converted to crystal temperatures. The experimental set up is shown schematically in Fig. 1 consisting of an encircling eddy current coil in a Hamco CG800 crystal puller. Silicon crystals were grown approximately 80 mm in diam from 6.5

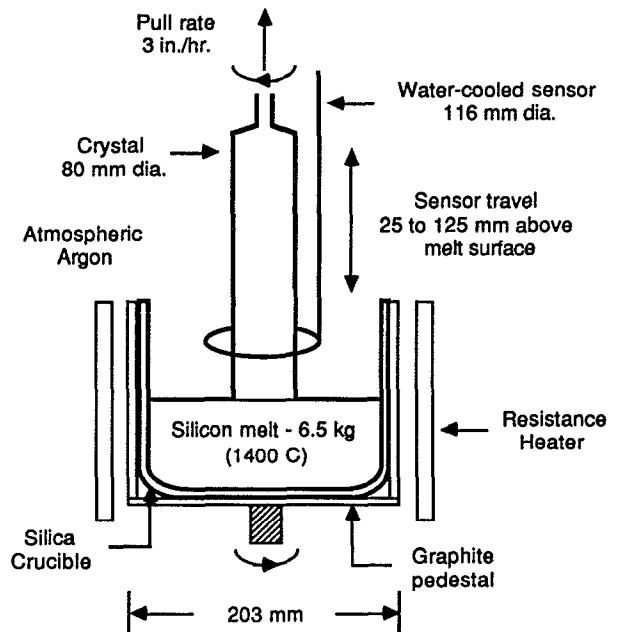


FIG. 1 Schematic showing the orientation of the encircling eddy current sensor in the Czochralski puller with respect to the growing crystal. The sensor is mounted through the top of the puller, and its axis is parallel to the growth axis. A feed-through assembly with a main lead screw and constant speed electric motor provides vertical travel of the sensor.

kg charges in 203 mm crucibles to lengths of 300–400 mm. Data were collected as the coil made vertical scans from 127 mm above the melt surface down to 25 mm above the melt at a constant velocity of 25 mm/min. This vertical scanning was repeated every 25 mm of crystal growth after the initial 100 mm of growth.

An analysis of the multifrequency eddy current data involved solving the electromagnetic boundary value problem of the field interacting with the crystal. A one-dimensional analytic solution and two-dimension finite difference solution with cylindrical symmetry of the governing electromagnetic wave equation derived from Maxwell's relations were employed to translate multifrequency eddy current response data into electrical conductivity values within the crystal. These electrical conductivities are then converted into temperatures.

Typical results for two of the growth runs in prior experiments are revealed in Figs. 2 and 3.<sup>4</sup> Here two-dimensional crystal isotherm plots are presented for crystals that have grown to a length of 250 mm. Isotherms are spaced 50 °C apart from the base line of 1400 °C for both the case of the reference run configuration (Fig. 2) and the case where the crystal was purposely cooled relative to the reference run by raising the initial exposed crucible position 25.4 mm, Fig. 3. These results indicate a crystal with a relatively hot center and significant radial thermal gradient at the levels well above the melt.

Derby and Brown's conduction heat transfer model calculations of relatively flat crystal isotherms for their reference configuration of Czochralski silicon growth are plotted in Fig. 4.<sup>5</sup> It is important to note that the isotherms in Figs. 2

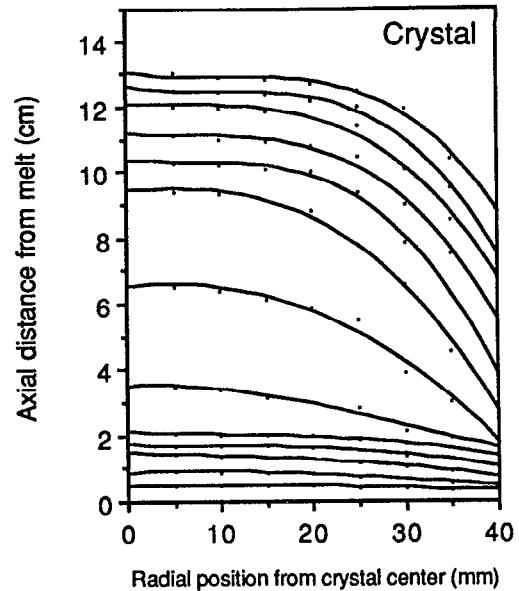


FIG. 3. This crystal isotherm plot for a 25.4 cm (10.0 in) crystal indicates that the crystal cools much more quickly relative to the reference run when the initial crucible position relative to the hot zone is raised 1 in. Again the isotherms are spaced 50 C apart from the base line of 1400 C. A cooler crystal is expected since when the crucible is raised, the crucible and graphite pedestal project out of the hot zone more. In this case the crucible loses more heat to the surroundings, i.e. the cold furnace walls. Consequently, less heat is directed towards the crystal, and the crystal cools.

and 3 at relatively large distances away from the crystal/melt interface, while showing roughly the same shape, are more sharply curved than the generally flat isotherms in the modeled data of Fig. 4.

The presence of these large radial gradients can, for ex-

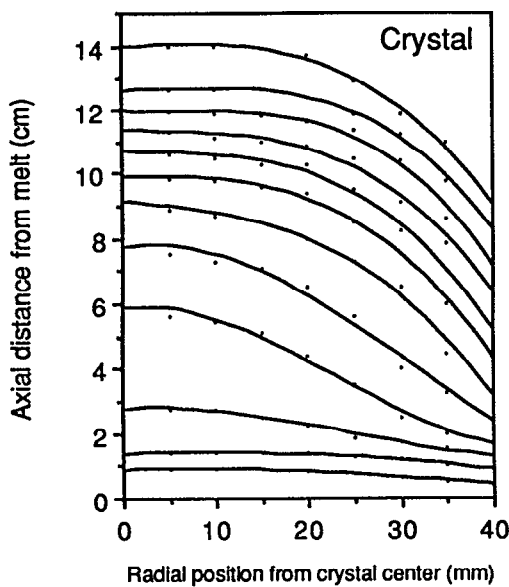


FIG. 2. The overall thermal character of the crystal is perhaps best revealed in an isotherm plot. Here crystal isotherms for a scan of the 26.0 cm (10.25 in) crystal during the reference run are presented. Axial symmetry is assumed. Isotherms are spaced 50 C apart from the base line of 1400 C (the crystal/melt interface). Significant radial gradients at relatively large axial distances from the melt are clearly revealed in this plot, estimated to be 7–8 C/mm near the crystal surface.

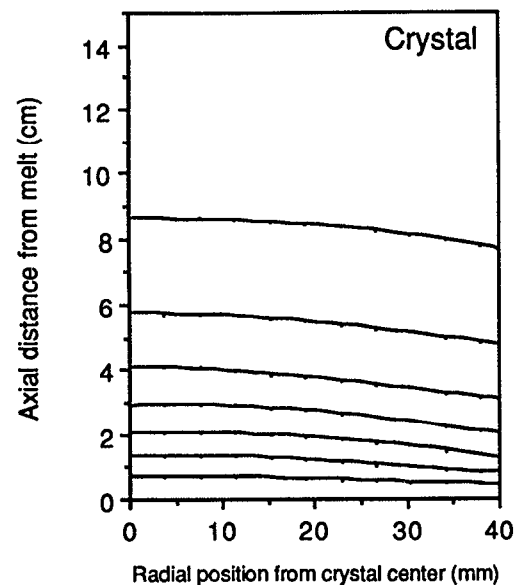


FIG. 4. Derby and Brown's calculations of crystal isotherms for a reference configuration of Czochralski silicon growth employing their thermal-capillary heat transfer model (see ref. 5). Here isotherms are spaced 60 K apart from the crystal/melt interface, the first curve above the base line. Compared to the relatively flat isotherms here in Fig. 4, the isotherms, in Figs. 2 and 3, at distances far from the melt, while showing roughly the same shape, are more sharply curved, indicating a hot-crystal center.

ample, significantly increase the thermal stresses induced in the growing crystal. Thus, if the transition temperature to optical transmission is a large fraction of the melting temperature of the material, the induced stress of radial thermal contraction will promote deformation and damage of the crystal through activated primary creep.<sup>6,7</sup>

For a relative comparison of transition temperature to transparency for different materials, one can calculate transition temperature from the material band gap energy. For example, the transition temperature  $T(x)$  for a semiconductor with a band gap of  $E_g(x)$  can be estimated to occur when the density of intrinsic carriers is the same as silicon when it becomes transparent. Where  $T(\text{Si})$  is the experimental temperature for silicon's onset of transparency and  $E_g(\text{Si})$  is the band gap of intrinsic silicon.

$$\begin{aligned} & [T(x)/T(\text{Si})]^3 \\ &= \exp(-E_g(x)/kT(x) \\ &+ E_g(\text{Si})/kT(\text{Si})). \end{aligned} \quad (1)$$

We will select 850 K as an arbitrary transparency temperature which corresponds to an optical depth of 1 mm at a wavelength of  $3.39 \mu\text{m}$  in silicon.<sup>8</sup> In Table I, Eq. 1 has been solved for some common semiconductors to determine the transparency temperature. The materials that would be most susceptible to primary creep damage are those with a ratio of absolute transition temperature to absolute melting point greater than 0.5,<sup>7</sup> which includes a list of crystal that are currently difficult to grow dislocation free.

The onset of transparency is gradual<sup>8</sup> as the number of free carriers decreases, and it is a function of the specific thickness of material that is being considered. This occurs over a range of temperatures but should become evident in the thermal profiles of the crystal when the surface region is cool enough to act as an efficient internal reflector. We expect a reflected flux of radiant energy to move up the crystal, being reabsorbed along the axis of the crystal. This will probably enhance the radial thermal gradient within the crystal and elongate the central high-temperature core.

In conclusion, the data suggest that for those materials which have an optical transparency transition temperature that is greater than one-half the melting temperature, infrared radiative transport within the crystal becomes increasingly important and must be considered in any modeling of the heat transfer process. Because large radial thermal

TABLE I. Transition Temperatures to Transparency,  $T(x)$

| Material | $n^a$ | Melt Pt.<br>K | Band Gap <sup>b</sup><br>eV | $T(x)$<br>K       | $T(x)/T_m.p.$ |
|----------|-------|---------------|-----------------------------|-------------------|---------------|
| Si       | 3.4   | 1693          | 1.11                        | 850 <sup>c</sup>  | 0.5           |
| Ge       | 4.0   | 1210          | 0.67                        | 450 <sup>d</sup>  | 0.37          |
| GaAs     | 3.2   | 1553          | 1.43                        | 1125 <sup>c</sup> | 0.72          |
| GaSb     | 3.7   | 978           | 0.69                        | 515 <sup>c</sup>  | 0.53          |
| InP      | 3.0   | 1343          | 1.28                        | 1015 <sup>d</sup> | 0.76          |
| AlSb     | 3.0   | 1323          | 1.60                        | 1350 <sup>d</sup> | > 1.0         |
| CdTe     |       | 1372          | 1.50                        | 1235 <sup>d</sup> | 0.9           |

<sup>a</sup> Refractive index see Ref. 9

<sup>b</sup> See Ref. 10

<sup>c</sup> See Ref. 8

<sup>d</sup> Estimate (Eq. 1)

gradients have been observed, it may be necessary to reduce the total rate of heat loss during growth in order to maintain low-radial thermal gradients and stresses.

The implications of these ideas on thin structures such as ribbons or films is determined by the length scale of the optical depth. Since the critical optical depth is a function of the material thickness this will force the effective transparency temperature to higher values and make dislocation-free processing for ribbons and fibers at elevated temperatures more difficult, even in silicon.

#### ACKNOWLEDGMENT

We thank IBM East Fishkill for financial support and technical assistance during this program.

<sup>1</sup> J. A. Stefani, J. K. Tien, K. S. Choe, and J. P. Wallace, *J. Cryst. Growth* **88**, 30 (1988)

<sup>2</sup> K. S. Choe, J. A. Stefani, J. K. Tien, and J. P. Wallace, *J. Cryst. Growth* **88**, 39 (1988)

<sup>3</sup> K. S. Choe, J. A. Stefani, J. K. Tien, and J. P. Wallace, *J. Cryst. Growth* **97**, 622 (1989)

<sup>4</sup> J. A. Stefani, Doctoral thesis, Columbia University (1988).

<sup>5</sup> J. J. Derby, and R. A. J. Brown, *Cryst. Growth* **74**, 605 (1986).

<sup>6</sup> T. Iwaki, and N. J. J. Kobayashi, *Applied Mechanics* **48**, 866 (1981).

<sup>7</sup> A. H. Cottrell, *An Introduction To Metallurgy* (St. Martin's, New York, 1967).

<sup>8</sup> K. I. Bilenko *et al.*, *Opt. & Spectrosc. (USSR)* **53**, 276 (1982).

<sup>9</sup> *Infrared Handbook* (edited by W. L. Wolfe and G. J. Aissis,) 7 (Office of Naval Research, Department of the Navy, Washington, DC, 1978).

<sup>10</sup> J. I. Pankove, *Optical Processes in Semiconductors* (Dover, New York, 1971).